ELSEVIER

Inorganica Chimica Acta 277 (1998) 193–201

Inorganica Chimica Acta

Potentiometric and NMR spectroscopic study of protonations and amide hydrogen exchange rates of DTPA-bis(butylamide), DTPA-bis(glucamide), and their lanthanide(III) complexes

Hendrik Lammers [a], Anna M. van der Heijden [a], Herman van Bekkum [a], Carlos F.G.C. Geraldes [b], Joop A. Peters [a,*]

[a] *Laboratory of Organic Chemistry and Catalysis, Delft University of Technology, Julianalaan 136, 2628 BL Delft, The Netherlands*
[b] *Department of Biochemistry, Faculty of Science and Technology and Center of Neurosciences, University of Coimbra, PO Box 3126, 3000 Coimbra, Portugal*

Received 13 June 1997; revised 5 September 1997; accepted 17 October 1997

Abstract

The macroscopic and microscopic protonations of DTPA-$GlucA_2$ (DTPA-bis(glucamide)) have been investigated using potentiometry, ^1H and ^{13}C NMR. The protonation behavior appears to be similar to that of the corresponding bis(alkylamides), showing that it is not affected by the presence of the polyhydroxy side chains. Consideration of the various possible protonation pathways leads to the conclusion that the differences in basicity of the amino functions in DTPA and DTPA-bis(amides) result in different protonation sequences of these ligands, which is reflected in the macroscopic protonation constants. The significance for the design of DTPA-based contrast agents for MRI is discussed. Exchange rates of the amide NH of this compound and that of DTPA-bis(butylamide) (DTPA-BuA_2) were determined via longitudinal relaxation rate measurements of the amide ^1H resonances in H_2O–D_2O (9:1) as solvent. The reaction is strongly base catalyzed and the rate increases substantially upon coordination of the DTPA-bis(amide) by La(III).

Keywords: MRI contrast agents; Lanthanide complexes

1. Introduction

Paramagnetic contrast agents are becoming increasingly important in biomedical diagnostics with the use of magnetic resonance imaging (MRI) [1–3]. About a third of the MRI scans are nowadays conducted after the administration of these agents [4]. Their action is based on the enhancement of the relaxation rates ($1/T_1$ and $1/T_2$) of water protons in the body, since these parameters contribute to the intensity of the MRI signal. Contrast agents allow, for example, an easier recognition of diseased tissue. The Gd(III) complexes of diethylenetriamine-*N,N,N',N'',N''*-pentaacetate (Gd(DTPA)$^{2-}$), 1,4,7,10-tetraazacyclododecane-*N,N',N'',N'''*-tetraacetate (Gd(DOTA)$^-$), and derivatives thereof are currently being employed in medical diagnosis. The fast evolution of the MRI technique has caused an increasing demand for more effective and more specific contrast agents.

Theory predicts that it should be possible to have contrast agents with relaxivities (relaxation rate enhancement per mM Gd(III)) that are 50 times higher than those of agents presently applied [3]. Design of contrast agents with higher efficacy requires fine-tuning of the various parameters that determine the relaxivity and, therefore, a thorough knowledge of structure–relaxivity relationships. An option to achieve a higher relaxivity involves the attachment of low molecular weight Gd(III) chelates to macromolecules such as polysaccharides [5,6]. The resulting contrast agents will have a prolonged residence time in the intravascular blood pool space and, therefore, may be useful in magnetic resonance angiography.

An important factor in the evaluation of contrast agents for MRI is the stability of these metal complexes under physiological conditions. Conditional stability constants at pH 7.4 are, in this regard, more meaningful than the thermodynamic stability constants [7]. Conditional stability constants can be calculated from the thermodynamic stability constants with the use of protonation constants. Since the thermodynamic stability of a Ln(III) complex of polyaminocarboxylate is related to the summed protonation constants of the free ligand [8,9], insight into structural effects on these constants is

* Corresponding author. Tel.: +31-15-278 5892; fax: +31-15-278 1415.

0020-1693/98/$19.00
PII S0020-1693(97)06151-3

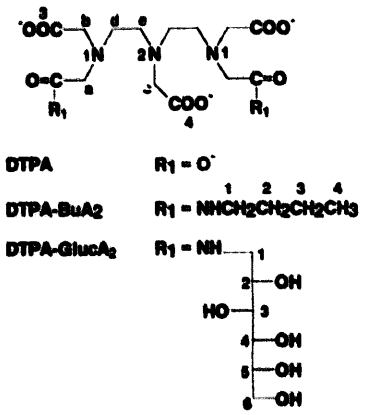

Fig. 1. Structures of compounds studied.

desirable. Previously, it has been reported that the second protonation constants of DTPA-bis(amides) are about 4 log units lower than those of the parent compound DTPA [10,11]. It was proposed that a possible explanation is the stabilization of some of the protonated forms by hydrogen bonding networks. In the present investigation, the macroscopic and microscopic protonation constants of DTPA-bis(butylamide) (DTPA-BuA_2, see structures in Fig. 1) and DTPA-bis(glucamide) (DTPA-$GlucA_2$) are studied in detail by means of potentiometry and measurements of the pH dependence of NMR shifts. The NMR measurements are conducted in a water–D_2O mixture (9:1, vol./vol.), to allow observation of the amide protons. The exchange of these protons between the amide group and water as a function of pH is investigated as well. The effects of coordination by La(III) on these parameters are evaluated. DTPA-$GlucA_2$ was included in this study because it can serve as a model compound for conjugates of DTPA and polysaccharides [12].

2. Experimental

2.1. Materials

Water used in the potentiometric titrations and in the NMR measurements was demineralized. All chemicals were purchased from Aldrich unless specified otherwise and were used without further purification. Lanthanum chloride was used as a mixed hydrate. The La(III) content was determined by complexometric titration with xylenol orange as the indicator [13]. The DTPA-bis(amides) DTPA-$GlucA_2$ [12] and DTPA-BuA_2 [10] were synthesized as described previously. La(III) complexes of these ligands were prepared by mixing solutions of equimolar amounts of hydrated $LaCl_3$ and ligand. The absence of free Ln(III) was verified using a xylenol orange indicator [13].

2.2. Potentiometry

Potentiometric titrations were conducted at 298 K in a double-walled vessel. The measurements were performed with a combined glass electrode, in which the 3 M KCl of the reference compartment was replaced by a saturated NaCl solution. Millivolt readings obtained were converted to pH values using a calibration curve, which was determined from standard buffer solutions. The ionic strength was maintained at 0.1 M using $NaClO_4$. The protonation constants were determined by titration of a 0.01 M ligand solution with 0.02 M HCl. Calculations for the potentiometric titrations were performed using a spreadsheet program described previously [14,15].

2.3. NMR measurements

^1H NMR spectra were recorded on Varian VXR-400 S NMR and Varian Unity 500 spectrometers with D_2O as the solvent and t-BuOH as the internal reference (δ (ppm): 1.20). The ^1H NMR pH titration curves and the amide hydrogen exchange rates of the bisamides and their La(III) complexes were measured with 0.04 M solutions in H_2O–D_2O (9:1, vol./vol.). The pH was adjusted to about 0 using 1 M HCl and subsequently raised to 12 in intervals of approximately 0.5 using diluted aqueous NaOH. The pH was measured with a calibrated Z11,344-1 Aldrich combination pH electrode. The values given are direct meter readings. ^{13}C NMR spectra were recorded on a Nicolet NT-200 WB, a Varian XL-200 NMR (50.3 MHz), or on a Varian VXR-400 S NMR spectrometer (100.6 MHz) using t-BuOH (δ (ppm): 31.2) as the internal reference. The ^{13}C NMR pH titration curves at 25°C were measured in a similar way as described for the ^1H NMR pH titration curves, but now using a 0.25 M solution of the ligand in D_2O. Longitudinal relaxation times (T_1) were measured with the use of an inversion recovery pulse sequence with a composite 180° pulse.

The complete spectral assignment of DTPA-$GlucA_2$ was carried out by means of ^1H homonuclear correlation spectroscopy (COSY) and ^1H–^{13}C chemical shift correlation spectroscopy (HETCOR).

The EXSY spectrum of DTPA-BuA_2 was recorded with a 0.04 M sample in H_2O–D_2O (9:1) as solvent, using a sweep width of 295 Hz centered around the amide ^1H signals (8.6–8.9 ppm). The mixing time was 0.3 s. Data were collected with 576 data points in F_2 and 24 data points in F_1. Pure absorption spectra were obtained by employing the States–Haberkorn method [16]. The obtained data matrix was zero-filled to 1024 × 1024 data points and processed using Gaussian weighting.

3. Results and discussion

3.1. Ligand protonation using potentiometry and NMR pH titration curves

The macroscopic protonation constants (log K_i) of DTPA-$GlucA_2$, as obtained with potentiometry, are given in Table 1. For comparison, previously determined data of DTPA-BuA_2

Table 1
Protonation constants for various DTPA-bis(amide) derivatives and DTPA in 0.1 M $NaClO_4$ at 25°C [a]

	log K_1	log K_2	log K_3	log K_4	log K_5
DTPA-GlucA_2 [b]	9.2	4.5	3.3	2.3	[d]
DTPA-BuA_2 [c]	9.2	4.5	3.2	[d]	[d]
DTPA [c]	10.2	8.6	4.2	2.9	1.8

[a] All values are within ±0.1. The protonation constants are defined as $K_i = [H_iL]/([H^+][H_{i-1}L])$.
[b] This work.
[c] Ref. [10], in 0.1 M NaCl.
[d] Not determined.

and DTPA [10] have been included. In general, three protonation constants for the DTPA-bis(amide) ligands as well as for DTPA can be determined using potentiometry. The log K_i values for DTPA-GlucA_2 are similar to those of other DTPA-bis(amides), showing that the sugar residues have no significant influence on the protonation of the DTPA moiety. Typically, these compounds have a log K_2, which is four units lower than that of DTPA.

Chemical shift titration curves of DTPA-BuA_2 and DTPA-GlucA_2 (see Fig. 2) display sharp changes of chemical shifts at pH values near the log K_i values. The positions of the inflection points agree with the potentiometrically determined protonation constants. The shapes of the ^{1}H chemical shift curves are similar to those of the previously studied DTPA-bis(alkylamides) [10]. A closer inspection of these curves shows that the ^{1}H chemical shifts for one of the terminal CH_2CO functions are almost pH independent for $6 < pH < 12$, whereas the other shows a pH jump of about 0.14 ppm at log K_1. We assign the latter CH_2CO signal to the amide methylene group, because a similar pH jump was not observed in the CH_2CO resonances of DTPA [10].

A quantitative estimate of the microscopic sites of protonation of DTPA-GlucA_2 and DTPA-BuA_2 was made with the ^{1}H NMR pH titration curves for the remaining protons in the DTPA backbone, following the empirical procedure of

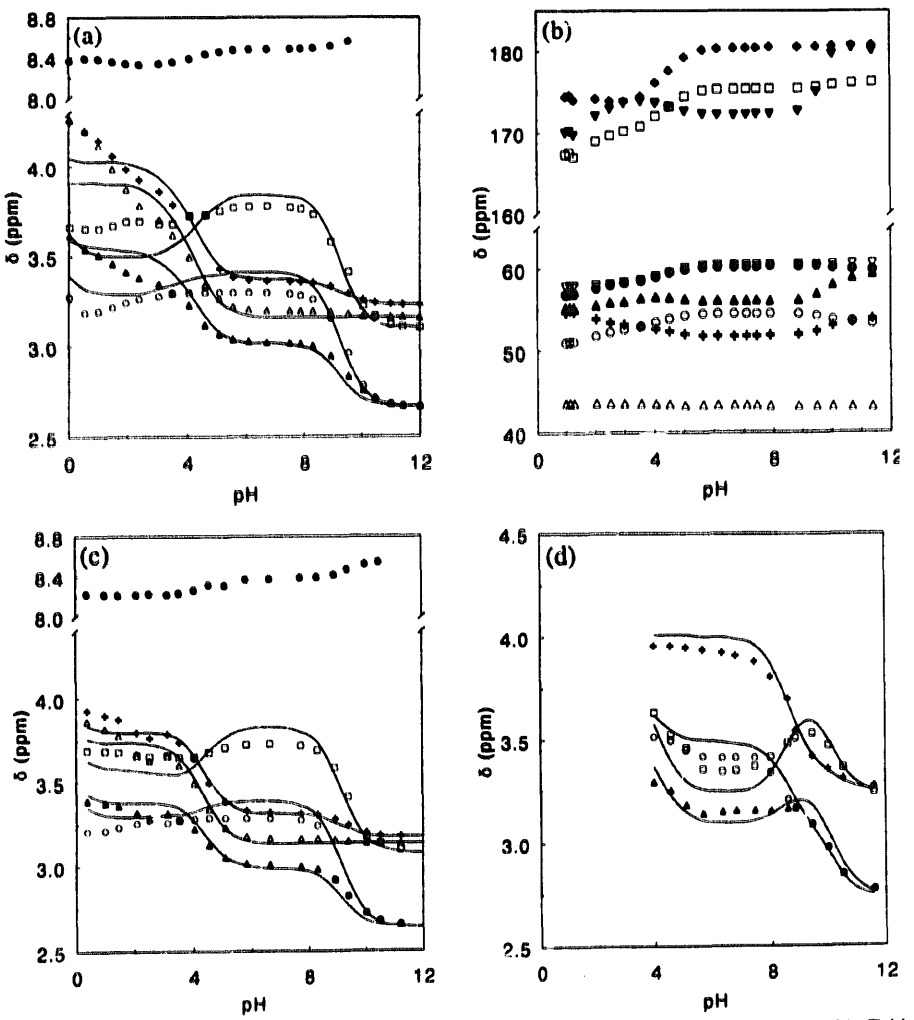

Fig. 2. Chemical shift titration curves at 25°C. The curves are calculated using the microscopic protonation constants listed in Table 4. For labeling of nuclei, see Fig. 1. (a) DTPA-GlucA_2 (^{1}H NMR, 400 MHz), CON*H* (●), H_a (+), H_b (△), H_c (□), H_d (▲), H_e (○). (b) DTPA-GlucA_2 (^{13}C NMR, 50 MHz), *C*OO(5) (◆), *C*OO(4) (▼), *C*ONH (□), C_a (●), C_b (▽), C_c (▲), C_d (○), C_e (+), C_f (△). (c) DTPA-BuA_2 (^{1}H NMR, 400 MHz), CON*H* (●), H_a (+), H_b (△), H_c (□), H_d (▲), H_e (○). (d) DTPA (^{1}H NMR, 200 MHz, Ref. [10]) H_a/H_b (+), H_c (□), H_d (▲), H_e (○). The assignment of H_d and H_e has been interchanged in Ref. [10].

Sudmeier and Reilley [17]. The protonation of amino or carboxylate groups in the DTPA backbone will result in a deshielding of the non-labile hydrogens and changes in chemical shifts indicate the site of protonation. The observed average chemical shift of nucleus i is given by $\delta^i_{obs} = \sum \delta^i_n X_{H_nL}$, where δ^i_n are the proton intrinsic chemical shifts of the H_nL species and X_{H_nL} is the mole fraction of each species. This equation can be rearranged to $\delta^i_{obs} = \delta_L + \sum V^i_n X_{H_nL}$ in which V^i_n is the chemical shift difference between H_nL and the unprotonated form L. Speciations at various pH values were calculated from the protonation constants obtained from potentiometry, the ligand mass balance and the equilibria equations. The V^i_n values were calculated for each set of shift data using a multiple linear regression program, which minimizes the sums of the squares of the deviation between the observed and calculated values δ^i_{obs}. The V^i_n values obtained for the various forms H_nL were then used to calculate the fractions of protonation of the nitrogen (N) and of the carboxylate (O) sites (f_N and f_O, respectively). The average number of ligand bound protons at all basic sites is $n = \alpha_N f_N + \alpha_O f_O$, where α_N and α_O are the number of equivalent N and O sites, respectively. It has been shown for linear poly(aminocarboxylate) chelates that the effects of protonation at various basic sites (V^i_n) are additive and can be calculated ($V^i_{n(c)}$) using [17]:

$$V^i_{n(c)} = \sum C_N f_N + \sum C_{N'} f_N + \sum C_{N''} f_N + \sum C_O f_O \quad (1)$$

where the pH-independent shielding constants $C_O = 0.20$, $C_N = 0.75$ and $C_{N'} = 0.35$ ppm can be used. The latter constants are the changes in proton chemical shift of the CH_2 groups under study, due to α-carboxylate protonation (C_O) or protonation of an N atom in the α-position (C_N) or in the β-position ($C_{N'}$). To account for the pH jump observed in the CH_2CONHR protons, a new shielding constant $C_{N''} = 0.14$ was included for the shielding of these protons upon protonation of the adjacent amino group. The values of f_N and f_O were calculated through minimization of the sum of the squares of the differences between the calculated and observed protonation shifts ($V^i_{n(c)}$ and V^i_n, respectively). In Table 2 the resulting values of f_N (f_1, f_2) and f_O (f_3, f_4) are compared with those obtained previously for DTPA [10].

Table 2
Percent protonation fractions of the different basic sites of DTPA-GlucA$_2$ compared with DTPA and various DTPA-bis(amide) derivatives for different values of n (for identification of f_i sites, see Fig. 1). The errors of f_i are ±5%

	n	f_1	f_2	f_3	f_4
DTPA-GlucA$_2$	1	4	89	0	2
	2	57	60	0	13
DTPA-BuA$_2$	1	5	87	0	2
	2	53	64	6	12
DTPA[a]	1	26	41	0	0
	2	87	16	0	5

[a] Ref. [10].

The data clearly show that the first protonation ($n = 1$) occurs predominantly at the central diethylenetriamine backbone nitrogen (f_2) for the DTPA-bis(amides), whereas in DTPA the central and the terminal nitrogen atoms have about equal basicity. Previously, it has been proposed that this difference in behavior and the large difference in log K_2 values between DTPA and DTPA-bis(amides) may be ascribed to stabilization of unprotonated and monoprotonated DTPA-bis(amide) species relative to the corresponding DTPA species, as a result of a bifurcated hydrogen bond between the amide hydrogen and the neighboring amine N and carboxylate [10,11].

To allow observation of the amide resonances, the present measurements were performed in a mixture of H_2O and D_2O (9:1, vol./vol.). The water signal was suppressed by presaturation with the transmitter in combination with a spin-echo pulse sequence. In this way a triplet for amide protons ($^3J = 5.6$ Hz) was observed at pH < 10. The linewidth of the amide proton increased between pH 6 and 10, indicating an increase in exchange rate upon raising the pH (see below). Above pH 10 the signal was no longer observable, probably because of excessive exchange broadening or by suppression of the amide resonance together with that of water because of very fast exchange between these protons. The chemical shift curves for the amide protons and the adjacent CH_2 function showed relatively small jumps at the various log K_i values (< 0.2 ppm). These may be ascribed to the protonations of the diethylenetriamine moiety or to disruption of intramolecular hydrogen bonds.

A quantitative evaluation of the ^{13}C NMR pH titration curves of DTPA-GlucA$_2$ (Fig. 2) was not possible, because the diethylenetriamine carbons showed downfield shifts upon protonation of one of the neighboring nitrogens. The ^{13}C protonation shifts for comparable carbon atoms in amino acids reported in the literature are usually positive [18–21]. Downfield protonation shifts have also been observed in ^{13}C shift curves for carbons in the diethylenetriamine backbone of DTPA [22,23]. Probably, the ^{13}C chemical shifts are more sensitive to conformational changes accompanying the protonation than ^1H shifts and, consequently, the common effects for the ^{13}C chemical shifts are no longer valid. The trends observed in the titration curves (Fig. 2), however, agree with the f values obtained from the evaluation of the ^1H data (Table 2).

The ^1H and ^{13}C chemical shifts of the sugar moiety of DTPA-GlucA$_2$ are almost independent of the pH (maximum variation of 0.07 ppm in ^1H shifts and 0.5 ppm in ^{13}C shifts between pH 0 and 12), showing that its hydroxyl groups are not involved in intramolecular hydrogen bonds with the DTPA backbone. Accordingly, the vicinal HH coupling constants (Table 3) are almost the same as those of sorbitol (D-glucitol) [24] and are independent of the pH. It can be concluded that the conformation of the sugar side chain is the same as that of sorbitol in solution, which is similar to the solid state structure.

Table 3
The proton coupling constants (Hz) of the sugar chain in DTPA-GlucA$_2$ [a] at 400 MHz and 25°C compared with those of sorbitol [b]

	$^2J_{1,1'}$	$^3J_{1,2}$	$^3J_{1',2}$	$^3J_{2,3}$	$^3J_{3,4}$	$^3J_{4,5}$	$^3J_{5,6}$	$^3J_{5,6'}$	$^2J_{6,6'}$
DTPA-GlucA$_2$	−14.0	4.0	8.0	5.5	2.3	8.0	3.0	6.0	−11.5
D-Sorbitol	−12.0	3.6	6.6	6.0	1.8	8.3	3.0	6.3	−11.8

[a] The carbon atom adjacent to the amide group has number 1.
[b] Ref. [24].

The ^{1}H NMR spectra of La(III) complexes of DTPA-GlucA$_2$ and DTPA-BuA$_2$ showed the presence of various isomers. Four well-separated amide signals were observed for La(DTPA-BuA$_2$) at pH < 8 (see Fig. 3). Previously, we have shown that DTPA-bis(amides) are coordinated by Ln(III) cations in an octadentate fashion via the three nitrogen atoms of the diethylenetriamine moiety, the three carboxylate oxygens, and the two amide oxygens [12,25]. The first coordination sphere is completed by a water molecule. The inversion of the three nitrogens of the diethylenetriamine unit is precluded upon coordination. Consequently, they become chiral in the complex and the ligand can occur in eight enantiomeric forms (four diastereomeric pairs). In the static situation, this would lead to eight signals for, for example, the amide hydrogens of La(DTPA-BuA$_2$). Two major dynamic processes play a role in the DTPA-bis(amides) [25–27]. Wagging of the ethylene units between two gauche conformations results in racemization at the central nitrogen atom. Furthermore, racemization of the terminal nitrogens is possible, but that requires decoordination of the concerning nitrogen and its adjacent COO$^-$ and amide CO functions. Consequently, the latter exchange process is relatively slow. The observation of four amide triplets in the ^{1}H spectra of DTPA-BuA$_2$ shows that the wagging motion is rapid on the NMR time scale. The exchange via racemization of the terminal nitrogen atoms was demonstrated by a two-dimensional EXSY spectrum (see Fig. 3). Each amide resonance has cross-peaks for exchange with two others, identifying the racemization at the two terminal amino nitrogens. No cross-peak is observed with the fourth isomer, obviously because that would require synchronous racemization of both terminal nitrogens. This exchange process is extremely slow because it requires decoordination of both terminal ends of the ligand. The NMR spectra of La(DTPA-GlucA$_2$) were more complex. Because of the chirality of the amide side chains, the number of resonances is twice as large here [12].

The resonances for the amide protons of these La(III) complexes broadened upon an increase of the pH and above pH 8 they were not observable. This can again be ascribed to the increasing rate of exchange between the amide hydrogens and bulk water. The chemical shifts were almost pH independent between pH 2 and 8. Upon a decrease of the pH below 2, all four amide resonances of La(DTPA-BuA$_2$) gradually shifted downfield (see Fig. 4) and decreased in intensity. The signals of the free ligand, however, were at an upfield position with respect of these signals. Therefore, this downfield shift cannot be explained by exchange between complex and free ligand. Most likely, this phenomenon is the result of protonation of the ligand, probably at the non-coordinated carboxylate oxygens. These spectra show the large stability of these La(III)-bisamide complexes under acidic

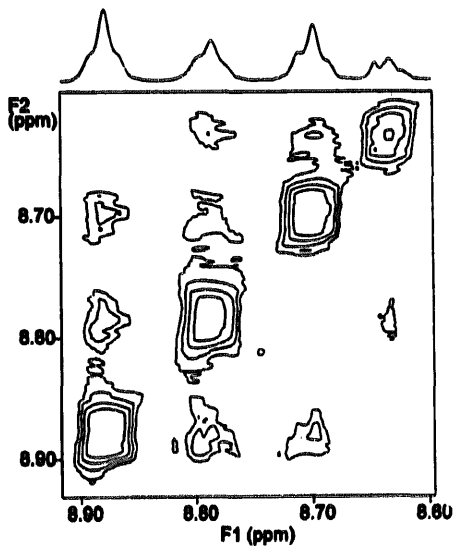

Fig. 3. 2D EXSY spectrum for the amide region of the ^{1}H spectrum of 0.04 M La(DTPA-BuA$_2$) in H$_2$O–D$_2$O (9:1, vol./vol.) at 25°C, pH 4.1 and 400 MHz.

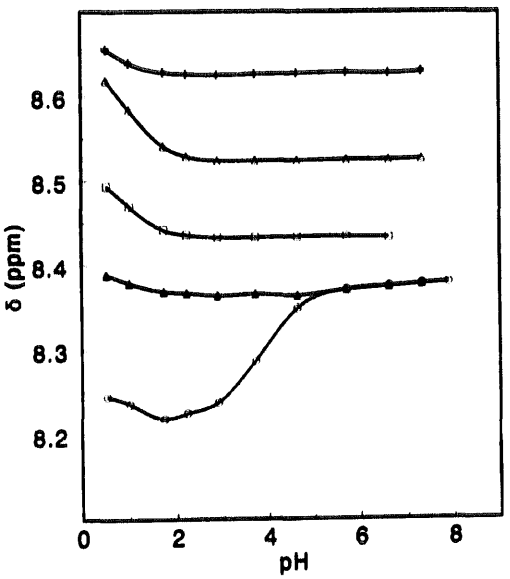

Fig. 4. ^{1}H chemical shift titrations of the amide region of 0.04 M La(DTPA-BuA$_2$) in H$_2$O–D$_2$O (9:1, vol./vol.) (+, △, □, ▲). An excess of free ligand (10 mol.%) (○) was present in the sample.

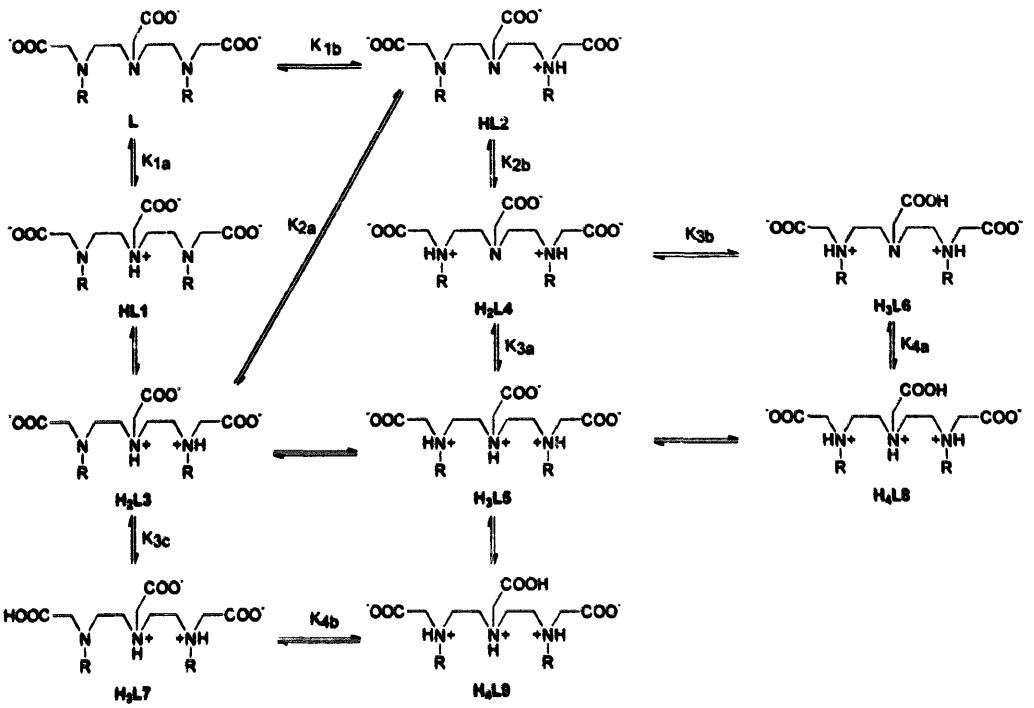

Fig. 5. Protonation sequences of DTPA and derivatives.

conditions, which is a result of the relatively low basicity of these ligands with respect to DTPA.

3.2. Protonation pathways of DTPA and its bis(amides)

The approach of Sudmeier and Reilley [17] for the analysis of chemical shift titrations of aminopolycarboxylates provides information on 'averaged' protonated species at various degrees of protonation. This analysis showed that the first protonation of DTPA takes place on both the central and the terminal nitrogens (see above); the basicities of these amino functions are about the same. After uptake of two equivalents of H^+, the protons reside predominantly at the terminal N-atoms. Microscopically, the picture is more complicated. In the monoprotonated species with the proton on the central N atom (HL1, see Fig. 5), the only possible second protonation is at a terminal N-atom giving H_2L3. However if the first proton is at a terminal N-atom (HL2), the second protonation can be either at the middle N-atom (H_2L3) or at the other terminal N-atom (H_2L4). The latter pathway is favored because it leads to less positive charge repulsion. An inspection of literature data shows that $\log K_1 - \log K_2$ for 1,4-diamines with chemically equivalent amino groups is generally in the range 2.8–4.0, whereas for 1,7-diamines $\log K_1 - \log K_2$ is only 0.6–1 [28]. Some typical examples are compiled in Fig. 6.

Changes in the basicity of an N-atom in DTPA by replacement of a neighboring carboxylate group by another group have a dramatic influence on the protonation pathways. From a comparison of reported log K values of nitrilotriacetic acid with derivatives in which one of the acetic acid moieties is substituted by an amide function (see Fig. 7), it may be expected that substitution of a terminal carboxylate by a carboxamide function leads to a decrease of the log K of the ammonium function of about 2.5 units [28]. This effect may be ascribed to the presence of a hydrogen bond between the amide NH and the amine nitrogen atom. Therefore, the central amino function of the DTPA-bis(amides) will be the most basic one and the initial protonation will occur predominantly at that atom (HL1). Then, the second protonation step leads to a relatively unfavorable diprotonated 1,4-diamine derivative (H_2L3). Consequently, the macroscopic protonation constant K_2 is dominated largely by this unfavorable step and will be relatively low, whereas in DTPA, the favorable protonation sequence, terminal N (HL2) → other terminal N-atom (H_2L4), will give rise to a higher value of K_2.

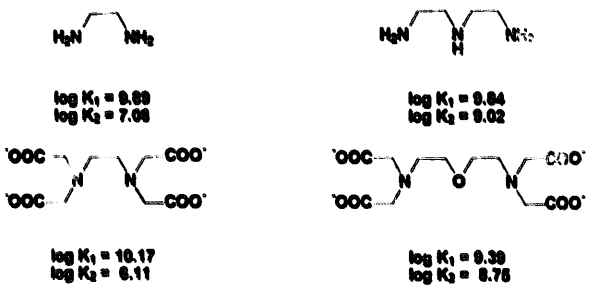

Fig. 6. Some examples of protonation constants of 1,4- and 1,7-diamines reported in Ref. [28].

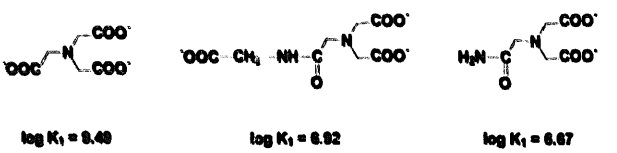

Fig. 7. Protonation constants of nitrilotriacetic acid and some derivatives [28].

The protonation equilibria that may play a role in the pH region of the chemical shift titrations are shown in Fig. 5. Too many protonation constants are involved in this model to allow for a useful fitting of the experimental data. Therefore, we have performed calculations of titration curves after including some arbitrary constraints. The value of $\log K_{1a} - \log K_{2a}$ was fixed at 2.8 and that of $\log K_{1b} - \log K_{2b}$ at 0.7. From a guess of the protonation constants the distribution of the various species was calculated [14,15]. Then, the (exchange-averaged) chemical shifts as a function of the pH were calculated from these concentrations and chemical shifts of the species estimated with the use of the pH-independent shielding constants for the various protonation sites (see above, Eq. (1)). In addition, the macroscopic protonation constants were calculated from the speciations. Subsequently, the deviation between the observed and calculated shifts and, simultaneously, the deviations between calculated and observed macroscopic protonation constants (Table 1) were minimized by variation of the microscopic protonation constants (see Table 4). The fits obtained are adequate (see Fig. 2); the calculated chemical shifts at pH > 2 are within 0.1 ppm of the observed ones, which agrees with the accuracy of the chemical shifts of model compounds calculated similarly by Sudmeier and Reilley [17]. The difference between the log K values of HL1 and HL2 for the DTPA-bis(amides) (see Table 4) agrees well with the value expected (2.7) based on a comparison of the log K_i values of nitrilotriacetic acid and corresponding carboxamides (see Fig. 7). It should be stressed, however, that these calculations merely serve to demonstrate that the proposed model may explain the NMR titration data. The microscopic protonation constants obtained should be treated with caution, because of the assumptions made during the fitting procedure and because of the inaccuracy of the shielding constants used for the estimation of the chemical shifts of the various species.

Table 4
Microscopic protonation constants[a] (log values) for various DTPA-bis(amide) derivatives and DTPA used to calculate the NMR titration curves in Fig. 2 (see text)

	DTPA	DTPA-GlucA$_2$	DTPA-BuA$_2$
K_{1a}	9.94	9.26	9.17
K_{1b}	9.69	6.99	6.97
K_{2a}[b]	7.14	6.46	6.37
K_{2b}[c]	8.99	6.29	6.27
K_{3a}	3.96	3.14	–[d]
K_{3b}	3.94	3.40	3.23
K_{3c}	–[d]	–[d]	3.17
K_{4a}	3.22	−0.31	−0.10
K_{4b}	−4.95	–[d]	–[d]

[a] Defined for the equilibria described schematically in Fig. 5. $K_{1a} = ([H][L])/[HL1]$; $K_{1b} = ([H][L])/[HL2]$; $K_{2a} = ([H][HL2])/[H_2L3]$; $K_{2b} = ([H][HL2])/[H_2L4]$ etc. (charges have been omitted for clarity).
[b] Fixed at $\log K_1 - 2.8$.
[c] Fixed at $\log K_2 - 0.7$.
[d] ≤ -5.

Protonation constants of many polyaminopolycarboxylates reported in the literature can be explained similarly. For example, bis(methyl)-DTTA (Fig. 5, R = CH_3, DTTA = diethylenetriamine-*N*,*N*′,*N*″-triacetate) has been reported to have $\log K_1$ and $\log K_2$ values of 10.70 and 9.09, respectively [29]. Replacement of a terminal acetate group of DTPA by a methyl group will result in an increase of the basicity of the terminal amino function concerned. Consequently, the initial protonation will occur preferentially at the terminal amino functions and the second protonation will be predominantly at the other terminal amino function, which minimizes the charge repulsion. Therefore, the value of $\log K_2$ is relatively close to that of $\log K_1$. If, on the other hand, the central acetate group of DTPA is replaced by a methyl group, $\log K_1$ and $\log K_2$ become 10.89 and 7.39, respectively [28]. Now, the central amino function is the most basic one and the population of the energetically unfavorable 1,4-diprotonated species (analogous to H_2L3) will be high, which is in line with the relatively large difference in protonation constants.

3.3. Kinetics of the exchange of the amide hydrogens with water

The kinetics of the amide hydrogen exchange was studied by the longitudinal ^1H relaxation rates, which were measured with the use of an inversion recovery pulse sequence with saturation of the water resonance during the acquisition and all delays. The magnetization recovery curves obtained are pH dependent and are single-exponential. As outlined by Zheng et al. [30], this suggests that the involvement of the amide hydrogen in a solvent-inaccessible hydrogen bonding is negligible or that the rates of opening and closing the hydrogen bonds are fast on the NMR time scale. This is supported by the signals for the methylene hydrogens of the acetate groups and the CH_2CONH functions, which both are singlets rather than AB systems as should be expected in case of restricted rotation due to hydrogen bonding [31,32]. In Fig. 8, the observed apparent longitudinal relaxation rates (R_1) for DTPA-BuA$_2$, DTPA-GlucA$_2$, and the corresponding La(III) complexes are plotted as a function of pH. The relaxation rates of the amide protons in the various isomers of the La(III) complexes were identical within the experimental error. If we assume that the Overhauser enhancement of the NH resonances by water saturation is negligible [33], the observed rate R_1 can be expressed as the sum of the intrinsic (dipolar) relaxation rate of the amide proton (R_n) and the exchange rate of the amide proton with water (k_{ex}):

$$R_1 = R_n + k_{ex} \quad (2)$$

The intrinsic relaxation rate of an amide proton is due to the dipolar relaxation of the NH with other H atoms in its proximity, which is pH independent. The upper limit of R_n can, therefore, be estimated from the minimum of the curves of R_1 versus pH. The data suggest that the exchange rates under neutral and acidic conditions are relatively low (of the same magnitude as or smaller than the intrinsic relaxation

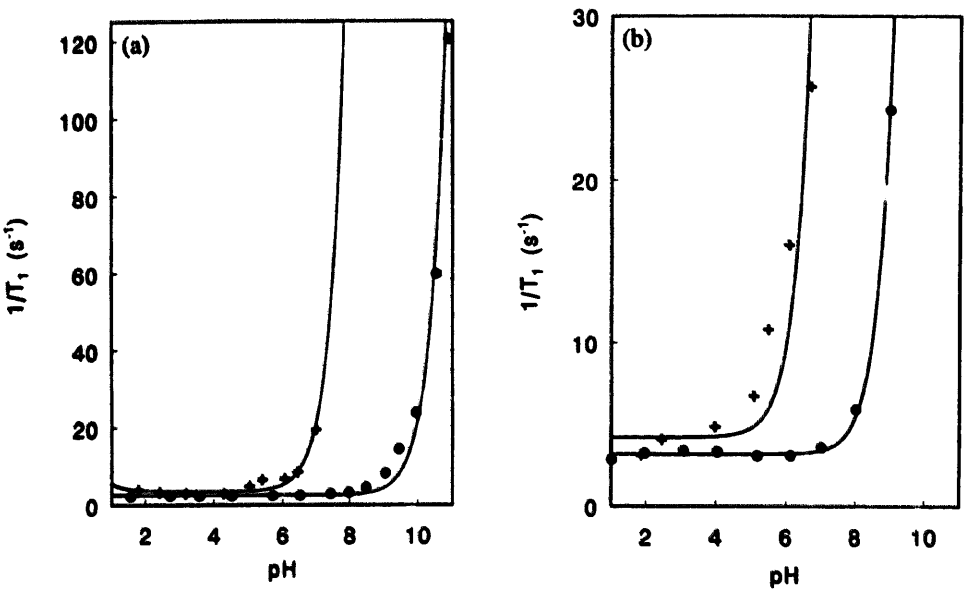

Fig. 8. Longitudinal ^1H relaxation rates as a function of pH for amide protons in (a) DTPA-BuA_2 and (b) DTPA-$GlucA_2$, and the corresponding La(III) complexes, measured in a 0.04 M solution in H_2O–D_2O (9:1, vol./vol.) at 25°C and 400 MHz. (●) Free ligand, (+) La(III) complex.

rates). Attempts to measure the exchange rates under those conditions by monitoring the integral of the resonance as a function of time upon dissolution of the compound into D_2O failed because the exchange was already complete before the first spectrum could be recorded (within 2 min). The lower limit of the exchange rates is, therefore, about 0.01 s^{-1}.

The exchange rates of NH protons commonly obey Eq. (3), where k_a, k_b, and k_w are the rate constants for catalysis by specific acid, specific base, and water [34]:

$$k_{ex} = k_a[H^+] + k_b[OH^-] + k_w \quad (3)$$

Combination with Eq. (2) gives Eq. (4), where $C = k_w + R_n$.

$$R_1 = k_a[H^+] + k_b[OH^-] + C \quad (4)$$

Fitting of the observed relaxation rates to Eq. (4) gives the rate constants shown in Table 5.

The exchange rates in DTPA-BuA_2 are lower than those in DTPA-$GlucA_2$. Probably, this is due to steric blocking effects of the aliphatic side chains. A similar effect has been observed in peptides [34]. The second-order rate constants for the DTPA-bis(amides) are somewhat smaller than those of *N*-methylacetamide [35] and model peptides with accessible NH groups (see Table 5) [34]. This may be explained by involvement of the amide protons in hydrogen bonds, reductions by one to six decades in exchange rates have been observed for protons involved in hydrogen bonding [36].

A substantial increase of the exchange rate is observed upon complexation to La(III), which can be ascribed to the decrease of the log *K* of the NH function because of the electron withdrawing effect of the metal ion. Enhancements of exchange rates of amide protons upon binding to metal ions have, for example, also been observed for polyglycine peptides [37]. If it is assumed that the acidity constants are controlled by the encounter-limited rate constant for the protonation of the amide anion by water (taken as 10^9 s^{-1} M^{-1}), it can be derived that log $K = 23 - \log k_b$ [38]. In this way the log *K* values of the amide functions are estimated to be 17.7, 16.7, 14.7, and 14.3 for DTPA-BuA_2, DTPA-$GlucA_2$, La(DTPA-BuA_2), and La(DTPA-$GlucA_2$), respectively.

Table 5
Rate constants for the exchange of amide hydrogens with water for some DTPA-bis(amides) in 0.04 M solutions in H_2O–D_2O (9:1 vol./vol.) at 25°C

	k_a (M^{-1} s^{-1})	k_b (M^{-1} s^{-1})	C[c] (s^{-1})	$R_{1,min}$[d]
DTPA-BuA_2	0.0	1.9×10^5	2.6	2.2
DTPA-$GlucA_2$	0.0	2.2×10^6	3.2	2.9
N-Methylacetamide [a]	3.6	4.2×10^6		
N-Acetyl-*N'*-methylamide [a]	4.6	1.7×10^7		
Poly-DL-alanine [b]	1.2	3.0×10^8		
La(DTPA-BuA_2)	21.2	1.8×10^8	3.4	2.9
La(DTPA-$GlucA_2$)	0	5.5×10^8	4.2	3.1

[a] Ref. [35], *N*-methylamide hydrogen exchange.
[b] Ref. [34], corrected for temperature difference.
[c] $C = k_w + R_n$ (see text).
[d] Upper limit of the intrinsic relaxation rate (R_n) of the amide proton.

Coordination of an amide oxygen by La(III) thus results in a decrease of the log K with 2.5–3 units.

In the paramagnetic Gd(III) complexes, which are potential contrast agents for MRI, the mobile NH protons can, in principle, contribute to the transfer of magnetization to the bulk water [3]. However, the observed exchange rates for this mechanism are much too low to be efficient.

4. Conclusions

The presence of the polyhydroxy side chains in DTPA-bis(amides) does not affect significantly either the macroscopic or the microscopic protonation of this ligand when compared with various DTPA-bis(amides) with alkyl side chains, such as DTPA-BuA_2. Therefore, the basicities and thus the affinities for metal ions of the amino functions in these ligands are similar. However, a significant difference exists between the DTPA-bis(amides) and DTPA with respect to the value of log K_2, which is substantially lower for the bis(amides). Previously, this has been ascribed to a stabilization of the non- and mono-protonated bis(amides) by bifurcated hydrogen bonds between the amide NH and the adjacent amino and carboxylate functions [10,11]. These phenomena result in a difference in preferred protonation pathways due to the decrease of the basicity of the terminal amino functions of DTPA. This may have important consequences for the design of DTPA-based contrast agents for MRI. It may be expected that derivatization of the parent compound so that the basicity of the terminal amino functions is enhanced with respect to that of the central one will lead to an increase of log K_1 and log K_2. Generally a linear correlation exists between $\Sigma\log K_n$ of polyaminopolycarboxylates and log β of their metal complexes. Therefore, it may be expected that the thermodynamic stability of the Gd(III) complexes increases upon the derivatization mentioned. Any derivatization that decreases the basicity of the terminal amino function of DTPA with respect to the central one will lead to a substantial difference between K_1 and K_2 (as in the DTPA-bis(amides)) and then, generally $\Sigma\log K_n$ and thus the thermodynamic stability of the corresponding metal complexes will decrease as well.

Acknowledgements

This investigation was carried out with the support of the Dutch National Innovation Program Carbohydrates, Akzo Nobel Central Research (ACR), the EC BIOMED 2 program (MACE project), and JNICT, Portugal (grant Praxis XXI 2/2.2/SAU/1194/95). The EC Erasmus program is thanked for funding the stay of A.M.v.d.H. at the University of Coimbra. This research has been done in the framework of the EC COST D1 program 'Synthesis and Physicochemical Studies of Lanthanide and Transition Metal Chelates of Relevance to Magnetic Resonance Imaging'.

References

[1] R.B. Lauffer, Chem. Rev., 87 (1987) 901.
[2] S.M. Rocklage, A.D. Watson and M.J. Carvlin, in D.D. Stark and W.G. Bradley (eds.), Magnetic Resonance Imaging, Mosby Year Book, St. Louis, MO, 2nd edn., 1992, Ch. 14.
[3] J.A. Peters, J. Huskens and D.J. Raber, Progr. Nucl. Magn. Reson. Spectrosc., 28 (1996) 283, and Refs. therein.
[4] R.C. Brasch, Radiology, 183 (1992) 1.
[5] R.C. Brasch, Magn. Reson. Med., 22 (1991) 282.
[6] P. Rongved and J. Klaveness, Carbohydr. Res., 214 (1991) 315.
[7] W.P. Cacheris, S.C. Quay and S.M. Rocklage, Magn. Reson. Imaging, 8 (1990) 467.
[8] G.R. Choppin, P.A. Bertrand, Y. Hasegawa and E.N. Rizkalla, Inorg. Chem., 21 (1982) 3722.
[9] G.R. Choppin, J. Less-Common Met., 11 (1985) 193.
[10] C.F.G.C. Geraldes, A.M. Urbano, M.C. Alpoim, A.D. Sherry, K.-T. Kuan, R. Rajagopalan, F. Maton and R.N. Muller, Magn. Reson. Imaging, 2 (1995) 13.
[11] D.H. White, L.A. DeLearie, T.J. Dunn, E.N. Rizkalla, H. Imura and G.R. Choppin, Inv. Radiol., 26 (1991) S229.
[12] H. Lammers, F. Maton, D. Pubanz, M.W. van Laren, H. van Bekkum, A.E. Merbach, R.N. Muller and J.A. Peters, Inorg. Chem., 36 (1997) 2527.
[13] G. Brumisholz and M. Randin, Helv. Chim. Acta, 42 (1959) 1927.
[14] J. Huskens, H. van Bekkum and J.A. Peters, Comput. Chem., 19 (1995) 409.
[15] J. Huskens, H. Lammers, H. van Bekkum and J.A. Peters, Magn. Reson. Chem., 32 (1994) 691.
[16] D.J. States, R.A. Haberkorn and D.J. Ruben, J. Magn. Reson., 48 (1982) 286.
[17] J.L. Sudmeier and C.N. Reilley, Anal. Chem., 9 (1964) 1698.
[18] J.G. Batchelor, J.H. Prestegard, R.J. Cushley and S.R. Lipsky, J. Am. Chem. Soc., 95 (1973) 6358.
[19] A.R. Quirt, J.R. Lyerla, Jr., I.R. Peat, J.S. Cohen, W.F. Reynolds and M.H. Freedman, J. Am. Chem. Soc., 96 (1974) 570.
[20] J.G. Batchelor, J. Feeney and G.C.K. Roberts, J. Magn. Reson., 20 (1975) 19.
[21] J.E. Sarneski, H.L. Suprenant, F.K. Molen and C.N. Reilley, Anal. Chem., 47 (1975) 2116.
[22] J.E. Sarneski, H.L. Suprenant and C.N. Reilley, Spectrosc. Lett., 9 (1976) 885.
[23] G.R. Choppin, S.A. Khan and G.C. Levy, Spectrosc. Lett., 13 (1980) 205.
[24] G.E. Hawkes and D. Lewis, J. Chem. Soc., Perkin Trans. II, (1984) 2073.
[25] C.F.G.C. Geraldes, A.M. Urbano, M.A. Hoefnagel and J.A. Peters, Inorg. Chem., 32 (1993) 2426.
[26] S.J. Franklin and K.N. Raymond, Inorg. Chem., 33 (1994) 5794.
[27] E. Bovens, M.A. Hoefnagel, E. Boers, H. Lammers, H. van Bekkum and J.A. Peters, Inorg. Chem., 35 (1996) 7679.
[28] A.E. Martell and R.M. Smith, Critical Stability Constants, Vols. 1, 2 and 5, Plenum, New York, 1974–1982.
[29] C. Paul-Roth and K.N. Raymond, Inorg. Chem., 34 (1995) 1408.
[30] Z. Zheng, M.R. Gryk, M.D. Finucane and O. Jardetzky, J. Magn. Reson. B, 108 (1995) 220.
[31] R.J. Day and C.N. Reilley, Anal. Chem., 36 (1964) 1073.
[32] R.J. Day and C.N. Reilley, Anal. Chem., 37 (1965) 1326.
[33] S. Waelder, L. Lee and A.G. Redfield, J. Am. Chem. Soc., 97 (1975) 2927.
[34] Y. Bai, J.S. Milne, L. Mayne and S.W. Englander, Proteins Struct. Funct. Genet., 17 (1993) 75.
[35] R.S. Molday and R.G. Kallen, J. Am. Chem. Soc., 94 (1972) 6739.
[36] S.W. Englander, N.W. Downer and H. Teitelbaum, Annu. Rev. Biochem., 41 (1972) 903.
[37] D.L. Rabenstein and S. Libich, Inorg. Chem., 11 (1972) 2960.
[38] H. Sigel and R.B. Martin, Chem. Rev., 82 (1982) 385.